

# Evaluation of *in vivo* THz Sensing for Assessing Human Skin Hydration

Hannah Lindley-Hatcher<sup>1</sup>, A. I. Hernandez-Serrano<sup>1</sup>, Jiarui Wang<sup>2</sup>, Juan Cebrian<sup>3</sup>, Joseph Hardwicke<sup>4</sup> and Emma Pickwell-MacPherson<sup>1</sup>

<sup>1</sup> Department of Physics, University of Warwick, Coventry, UK

<sup>2</sup> Department of Electronic Engineering, Chinese University of Hong Kong, Shatin, Hong Kong

<sup>3</sup> Lipotec SAU, Barcelona, Spain

<sup>4</sup> University Hospitals of Coventry and Warwickshire NHS Trust; and Warwick Medical School, University of Warwick, Coventry, UK

E-mail: [e.macpherson@warwick.ac.uk](mailto:e.macpherson@warwick.ac.uk)

Received xxxxxx

Accepted for publication xxxxxx

Published xxxxxx

## Abstract

Terahertz (THz) *in vivo* reflection imaging can be used to assess the water content of the surface of the skin. This study presents the results of treating 20 subjects with aqueous, anhydrous and water-oil emulsion samples and observing the changes induced in the skin using THz imaging. These regions were also measured with a corneometer, the present gold standard for skin hydration assessment within the cosmetics industry. We find that THz imaging is effective at observing the presence of oil and water on the surface of the skin, these results can be verified with the measurements of capacitance taken by the corneometer. The THz measurements reveal a distinction between the responses of subjects with initially dry or well hydrated skin, this observation is particularly noticeable with the oil-based samples. Additionally, moderate correlation was found between the THz reflected amplitude and capacitance of untreated skin with a correlation coefficient of  $r = -0.66$ , suggesting THz imaging has promising potential for assessing skin hydration.

Keywords: Terahertz, time-domain spectroscopy, *in vivo* imaging, moisturisers, corneometry, capacitance

## 1. Introduction

Terahertz time-domain spectroscopy (THz TDS) is being studied in the context of an increasing number of biomedical applications, as its strong sensitivity to water and non-ionizing nature make it desirable for use in studying living tissues [1]. Successful *in vivo* studies have been performed including the diagnosis of diabetic foot syndrome [2], evaluating the healing process of scars [3], studying the efficacy of silicone gel treatments to rehydrate damaged skin [4], and assessing corneal hydration [5]. Additionally, *ex vivo* studies have shown promising results with potential for: cancer diagnosis [6] [7] [8]; quantifying the effect of different approaches to transdermal drug delivery [9]; and looking at the interactions of different moisturiser ingredients with the skin [10].

These aforementioned applications are possible due to the sensitivity of THz light to water caused by the high absorption coefficient of water at THz frequencies [11]. This is, however, a double-edged sword as the high absorption also limits the penetration depth in living tissues. This restricts many *in vivo* studies at present to studying areas such as the skin or the eye, which can be accessed using a THz reflection system without passing through other regions of high water content.

An additional consequence of the sensitivity of THz light to water content is that subtle changes in the skin can alter the THz response. For example, it has been shown that occlusion of the skin prevents natural water loss, causing water to build up in the stratum corneum (SC) altering the hydration profile [12]. Also, variations in the contact pressure between the skin and a surface change the compression of the tissue and affect the THz response [13]. Studies have also shown that circadian rhythms can affect the skin barrier function [14]. As

understanding of these effects increases, experimental protocols and processing techniques can be developed to reduce and remove their influence on the results, making it possible to obtain repeatable results that are comparable between different subjects [15].

Lindley-Hatcher *et al.* developed a robust protocol which can be used to obtain repeatable results for the THz response of skin following treatment with a commercially available moisturiser on a single subject. In order to further verify the application of THz imaging to *in vivo* hydration assessment it is necessary to compare the results to an alternative technique. The corneometer is an accepted gold standard for quantifying the effect of different skin treatments on the SC hydration [16]. According to the web of science there have been 287 publications referring to the corneometer produced between 1987 and 2020; many of these use the measurements to demonstrate the efficacy of the new sample or a new device for skin measurements.

In order to offer a thorough comparison of the two devices, three common moisturiser components are tested on 20 subjects and the changes in the reflected THz signal and skin capacitance are compared. This is the first comprehensive comparison of *in vivo* THz imaging of the skin with capacitance skin measurements and makes it possible to assess the ability of THz imaging to diagnose the state of the SC hydration.

It has previously been demonstrated that THz measurements of the skin have the potential to provide more quantitative information about the hydration profile of the skin than can be obtained by a corneometer [17]. Additionally, there are known weaknesses of the corneometer including its lack of specificity to skin water content and the limited ability to link the measured result to changes in the skin both of which we anticipate THz sensing will be able to overcome. Furthermore, the cost and size of THz systems are decreasing and we envisage THz sensing will become affordable for many future applications including high precision diagnosis and evaluation of skin conditions leading to the prescription of more effective treatment options.

## 2. Theory

### 2.1 Techniques to Study Human Skin Hydration

#### 2.1.1 Terahertz Measurements

For this study a reflection geometry THz system is used, where the THz signals reflected from the surface of the skin are analysed to learn about the interfaces that cause the reflections. Following the Fresnel equations, the reflection coefficient  $r_{12}$  for s polarized light at an interface can be written in terms of the refractive indices of the media involved, as shown in equation 1:

$$r_{12} = \frac{\tilde{n}_1 \cos \theta_i - \tilde{n}_2 \cos \theta_t}{\tilde{n}_1 \cos \theta_i + \tilde{n}_2 \cos \theta_t}, \quad (1)$$

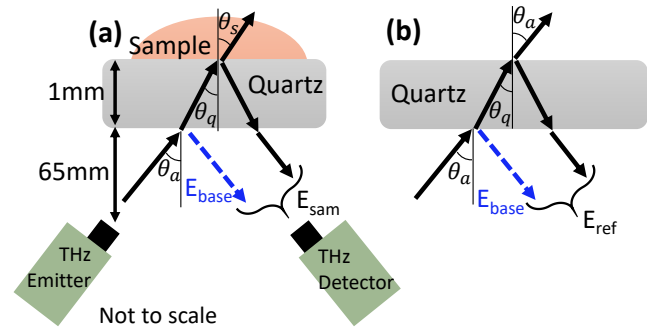


Figure 1. A schematic for THz reflection imaging (a) acquiring the sample measurement, (b) acquiring the air reference. The baseline reflection from the lower surface of the quartz is shown by the dashed blue lines in both figures. (a) includes dimensions of the system and the locations of the THz probes.

where  $\tilde{n}_1$  and  $\tilde{n}_2$  are the complex refractive indices of the media and  $\theta_i$  and  $\theta_t$  are the angles of the incident and transmitted waves respectively. In the reflection geometry shown in figure 1, with the skin in contact with a quartz window to aid alignment, there are two reflections; one from the lower surface of the quartz known as the baseline,  $E_{base}(t)$ , and one from the upper surface. Measurements are taken of the sample in contact with the quartz window,  $E_{sam}(t)$ , and additionally of the quartz with no sample to act as an air reference,  $E_{ref}(t)$ . To obtain the sample to reference ratio  $M_{meas}$  from the measured pulses, the baseline must be subtracted from the sample and reference measurements using the approach developed by Chen *et al.* [18], as shown in equation 2:

$$M_{meas} = \frac{FFT(E_{sam}(t) - E_{base}(t))}{FFT(E_{ref}(t) - E_{base}(t))}, \quad (2)$$

here the Fourier transform is taken so that the data can be studied in the frequency domain. The ratio of the sample to reference pulses can also be expressed theoretically  $M_{theo}$ , as summarised by equation 3,

$$M_{theo} = \frac{r_{qs}}{r_{qa}} = \frac{\tilde{n}_q \cos \theta_q - \tilde{n}_s \cos \theta_s}{\tilde{n}_q \cos \theta_q + \tilde{n}_s \cos \theta_s} \times \frac{\tilde{n}_q \cos \theta_q + \tilde{n}_a \cos \theta_a}{\tilde{n}_q \cos \theta_q - \tilde{n}_a \cos \theta_a}. \quad (3)$$

Where  $\theta_q$  is the incident angle of the THz radiation inside the quartz and  $\theta_s$  and  $\theta_a$  are the transmitted angles of the THz radiation inside the sample and in air as marked in figure 1. The ratio of the reflected signals is written mathematically using the Fresnel coefficients for the quartz-sample and quartz-air interfaces,  $r_{qs}$  and  $r_{qa}$  respectively. Using equation 1 these coefficients can be expressed in terms of the refractive indices of quartz, air and the sample  $\tilde{n}_q$ ,  $\tilde{n}_a$  and  $\tilde{n}_s$ . By equating  $M_{meas}$  to  $M_{theo}$  and rearranging equation 3, the unknown refractive index of the sample,  $\tilde{n}_s$ , can be found [18].

In addition to considering the frequency dependent parameters which can be extracted from the sample, the time domain signal can also be studied. The standard processing technique for THz reflection spectroscopy is to remove the

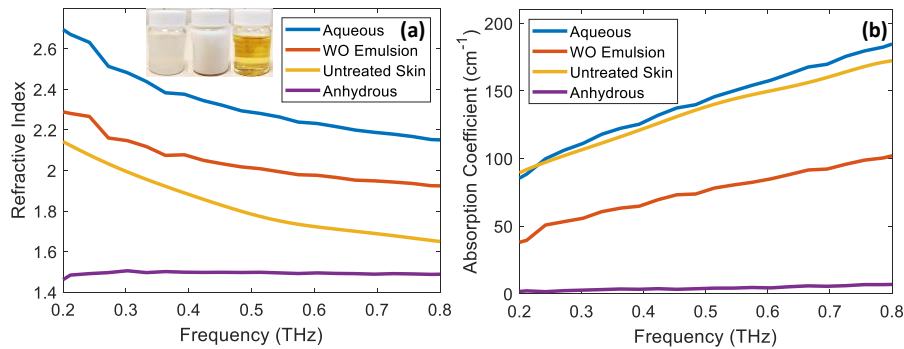


Figure 2. (a) The refractive indices of each sample as measured in a transmission geometry and a refractive index profile for untreated skin measured in reflection geometry. Inset: from left to right images of the aqueous, WO and anhydrous samples used in the study. (b) The absorption coefficient of each of the samples measured as above, with the profile of untreated skin measured in reflection included for reference.

effects of the baseline mentioned above. The key equation defining the processed signal  $S$  is given by equation 4 [12]:

$$S = iFFT[FFT(filter) \times M_{meas}]. \quad (4)$$

In this work we used a double Gaussian filter to remove low and high frequency noise within the signal, with 0.1 and 0.6 THz being used as the low and high frequency thresholds respectively. The result is a smooth impulse function representing the signal reflected from the sample; the amplitude of this processed signal can be used to quantify changes in the skin.

The amplitude of the reflected signal depends on the contrast between the refractive indices of the quartz window and the sample, as it is proportional to the reflection coefficient  $r_{qs}$ . It can be seen that as the difference between the refractive indices of the two layers increases the reflected amplitude increases. In previous studies it has been shown that for a quartz-sample interface, a decrease in the reflected amplitude can be interpreted as an increase in the water content of the skin, as more hydrated skin has a higher refractive index, closer to that of quartz [17]. This theory can be extended further to a wider range of changes that may be induced in the skin following treatment with samples such as oil.

The individual samples were measured in the transmission unit of the TeraPulse 4000 THz TDS system (TeraView Ltd, Cambridge), described in section 3.3. A liquid cell was used in which the samples were sandwiched between two pieces of quartz each 3mm thick using a 0.1mm spacer. We present the results for the samples measured in transmission for the frequency range 0.2-0.8 THz to correspond to the usable frequency range for the frequency dependent properties of skin calculated from measurements obtained using a reflection geometry with this system.

In this study the samples contained common components of commercial moisturisers, the ingredients of the samples can be seen in Table 1. The extracted refractive indices and absorption coefficients of the samples can be seen in figure 2,

the mathematical technique used is described by McIntyre et al. [19].

As an example, figure 2 (a) shows the extracted refractive index from a single measurement of untreated human skin taken *in vivo* using the standard reflection geometry. The refractive indices of the aqueous and WO (Water in Oil) samples are larger than that of skin, therefore if these samples are present on the skin surface the refractive index will increase and will be closer to the refractive index of the quartz window ( $\tilde{n}_{quartz} = 2.12 - 0i$ ) [20], reducing the reflection coefficient. However, if the anhydrous sample is applied to the skin and remains on the surface the refractive index will reduce, this will increase the contrast between skin and the quartz window, increasing the reflection coefficient. Using these initial measurements, it is possible to make predictions about the change in the THz response of skin following treatment with these different samples. However, it is also

TABLE 1

INCI <sup>a</sup>	WO Emulsion	Aqueous System	Anhydrous	Ingredient Effect
Water	qs100	qs100		
Triolein	30%		99%	Emollient, occlusive
Glycerine	10-12%	10-12%		Humectant, NMF <sup>b</sup>
Phenoxyethanol	0.5%	0.5%		Stabiliser
Polyglyceryl-3 Polyricinoleate	2%			Stabiliser
Methyl Glucose Dioleate	2%			Emulsifier
Sphingomonas Ferment Extract		0.3%		Occlusive, humectant
Caprylic/Capric Triglyceride	1%		1%	Occlusive

<sup>a</sup>International Nomenclature of Cosmetic Ingredients, <sup>b</sup>Natural Moisturising Factor.

A list of the compositions of each sample tested in this study, and a summary of the expected effects of this ingredient on the skin.

expected that this response will vary between subjects and will depend on how well the sample is absorbed into the skin, as well as the initial refractive index of the skin.

For completeness figure 2 (b) shows the extracted absorption coefficients of each of the samples, however there are minimal changes observed in the absorption coefficient of the skin following the application of the samples. In the model of the skin used to extract these properties, the effects of scattering are neglected as they are negligible due to the sizes of the particles within the samples being sufficiently small compared to the wavelengths used in this study.

### 2.1.2 Corneometer Measurements

The capacitance of the surface of the skin is measured using a corneometer, which can be used to infer the relative hydration. Tracks of oppositely charged gold plates are interleaved on the head of the electrode, resulting in a shallow electric field that penetrates into the upper layers of the skin. This measurement can be used to infer the dielectric properties of the skin surface which are correlated to the hydration [21].

The measurements taken by the corneometer are in standard corneometer units which give a scaled measurement of the capacitance of skin. The range of these values is from 0, which is calibrated as the response where there is no water in the sample, to 120, which is calibrated with pure water [22]. It is possible that if an oily sample is used on the skin and leaves a residue, the response measured may be smaller than expected due to interference caused by the film [23].

## 2.2 The Stratum Corneum

### 2.2.1 The Function of the Stratum Corneum

The primary function of the skin is to form a semi permeable protective barrier capable of maintaining the required hydration levels inside the body and preventing harmful chemicals from entering. This barrier allows water to enter and leave the body at a controlled rate, some water will be absorbed through washing whilst water can be lost through a process called Transepidermal Water Loss (TEWL). If the skin barrier is healthy this TEWL is controlled, however if there is damage to this barrier the skin can dry out [24].

### 2.2.2 Percutaneous Absorption

As the SC is semi permeable, substances can enter the body via the skin, in a process known as percutaneous absorption. Many factors can contribute to the rate of percutaneous absorption including skin hydration, skin health, barrier function and external factors such as washing or exfoliating [25]. Studies have been performed investigating links between percutaneous absorption and skin hydration, and it has been found that excessive hydration can increase absorption as soluble components of the sample can diffuse through the SC more easily [26]. However, poor skin barrier function, which is often linked to dry skin conditions, can also increase absorption rates [27]. One study using normal and cosmetically dry skin to test the difference in barrier function found that the barrier function of normal skin is 40% higher than that of dry skin [28]. This means that naturally dry skin is likely to have higher rates of percutaneous absorption than initially well hydrated skin; this may influence how these different skin types respond to the applied samples.

### 2.2.3 Response of the Skin to Different Samples

Table 1 shows the three samples tested in this study, their compositions, and the effects that each ingredient is anticipated to have. The three sample types applied in this study are: an aqueous sample primarily consisting of water and glycerine; an anhydrous sample containing triolein and a WO emulsion which is a mixture of both the samples.

An increase in the presence of water is expected to increase the corneometer measurement, but any residue of oil components can interfere with this measurement, decreasing the measured value of skin capacitance. An increase in skin hydration is expected to decrease the THz reflectivity, as the refractive index of skin is brought closer to that of quartz. However, oil on the surface of the skin will increase the THz reflectivity as the difference in the refractive indices will increase.

Figure 3 shows the mechanisms through which each of these samples are expected to interact with the skin to increase the hydration. The aqueous sample is shown in figure 3(a), and the main effect arises from the absorption of water and glycerine. Glycerine acts as a humectant meaning that it is able

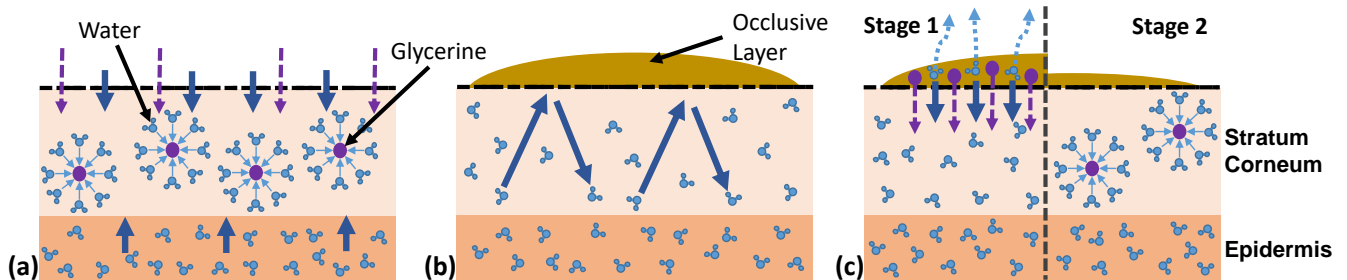


Figure 3. The mechanisms of the interactions of (a) the aqueous sample, (b) the anhydrous sample and (c) the WO sample with the skin. The blue and purple arrows show the movement of water and glycerine respectively.



to draw water to itself and bind to it [29]. Therefore, this aqueous sample draws water into the SC from the sample and potentially from deeper layers of the skin which are more hydrated. When glycerine is applied to the skin with water it can reduce the diffusivity of water, reducing the rate at which this absorbed water is lost from the surface of the skin [30]. The absorbed water is therefore held in place by the glycerine, increasing the hydration of the SC [31].

The anhydrous sample acts as an emollient softening the skin and also forms an occlusive layer on the surface of the skin. The effects of this occlusive layer are demonstrated in figure 3(b); the oil on the skin surface forms a water-proof barrier which traps water inside the skin allowing the SC hydration to increase [32]. It is possible that the formation of this occlusive layer on the surface of the skin could interfere with the corneometer measurement making it appear that the skin hydration has not significantly increased. It is expected that on the short timescales being used for this study with just one measurement 20 minutes after treatment, the presence of oil on the surface of the skin will be visible in the THz response of skin as the reflected amplitude will increase.

The interaction of the WO emulsion is shown in figure 3(c) as a two stage dynamic process which is a combination of the mechanisms seen in the two other samples. It is understood that initially the water component of the sample will be absorbed into the skin and some will evaporate from the SC (on a timescale of approximately 15 minutes). This will leave the oil components behind on the surface of the skin in what is known as the lipidisation phase [33]. At the point 20 minutes after the treatment when the measurement is performed it is expected that the oil components will dominate the measurement.

### 3. Methodology

#### 3.1 Protocol

20 subjects were studied for the purposes of this investigation (9 males, 11 females) of ages ranging from 21-52. All volunteers gave informed consent to be involved in the study. The protocol for this study is summarised by table 2. All subjects were measured on the same day to minimise variations caused by external factors such as climate. Each region of the skin was measured with both techniques before treatment with any products, making it possible to normalise the observed changes in the treated regions to the initial state of the skin and account for any natural variation. Four regions were marked on the arms, three on the left arm to be treated and one on the right arm to remain untreated acting as the control, these regions are shown in figure 4(b).

After the initial measurements of the skin the regions were treated with anhydrous, aqueous and WO samples. The sample volume of 0.036 ml was measured using a micropipette and applied to each region before being rubbed in by the subject

TABLE 2	
(a)	Subject enters the lab
(b)	Acclimatise to controlled environment for 20 minutes, $T = 23^{\circ}\text{C}$
	Mark four 3cm x 3cm regions on the volar forearms
	Measure the regions with the corneometer and the THz system
	Apply 0.036ml of a sample to the corresponding region
	Wait 20 minutes for sample to be absorbed
	Repeat measurements with both techniques

Figure 4. (a) Corneometer used to take capacitance measurements of the skin, (b) regions to be measured marked on the volar forearm. Table 2 lists the protocol employed to take the measurements in this study.

whilst wearing a latex glove. This prevented the sample being absorbed by the hand used to rub it in. The subjects then waited 20 minutes for the samples to be absorbed. Following this the four regions were then measured again with both techniques.

#### 3.2 Capacitance Measurements

Capacitance hydration measurements of the skin were taken using a Corneometer CM825 (Courage+Khazaka Electronic, Cologne, Germany) [22], shown in figure 4(a). The probe was wiped with a dry tissue between each measurement to remove any residual sample remaining on the skin surface or other skin surface lipids which could interfere with the next measurement.

The measurement with the corneometer is linked to a spring based pressure system, which ensures that the probe is applied to the skin with the desired pressure of 1 N before the measurement is taken [22]. Once the desired pressure has been reached the measurement is taken which lasts less than one second.

#### 3.3 Terahertz Measurements

Point scans of each region were acquired in a reflection geometry using THz light generated and detected using a TeraPulse 4000 system (TeraView Ltd, Cambridge), shown in figure 5(a). This system produces broadband pulses in the range from 0.06-5 THz. Due to the high absorption coefficient of the water which is a primary component of the skin we are only able to use data within the frequency range 0.2-0.8 THz to study the skin. The incident angle of the THz beam onto the quartz window was  $30^{\circ}$ .

Many variables can have an impact on the THz response of the skin, including occlusion and pressure. Therefore the protocol proposed by Lindley-Hatcher *et al.* [15] was closely followed, and a pressure sensor system was used to enable

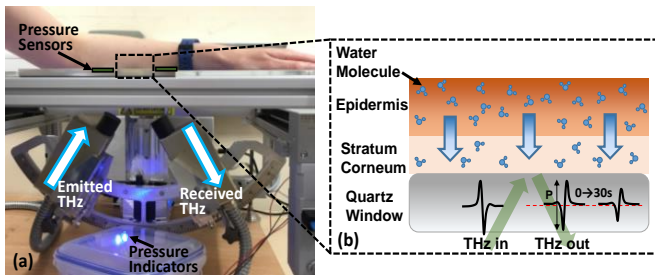


Figure 5. (a) The experimental setup to take *in vivo* measurements of the skin using THz radiation in a reflection geometry, combined with pressure sensors and indicator lights to improve repeatability of the measurements. (b) The effects of occlusion caused by the quartz window on the skin, water builds up in the stratum corneum and the amplitude of the measured THz pulse decreases due to an increased water content. P marks the peak-to-peak amplitude of the reflected signal.

repeatability. The pressure sensor allows the subject to observe whether the pressure applied is in the correct range of  $1.6\text{--}2\text{ N cm}^{-2}$  and make real time adjustments. This pressure range is chosen so as to be low enough that all subjects are comfortable in maintaining the pressure for the duration of the measurements, whilst high enough to ensure that there is no air gap between the skin and the quartz window [13]. The information from the pressure sensor is exported along with the THz data: this makes it possible to exclude data points recorded at the incorrect pressure.

To study the dynamic response of skin, 200 measurements were recorded in 33 seconds with an acquisition rate of 30 Hz and five waveforms were averaged to complete a single measurement. For the duration of the measurement the skin is occluded by the quartz window which causes the hydration profile of the skin to change, as illustrated by figure 5(b). The rapid sampling rate chosen makes it possible to not only observe the initial state of the skin at the start of occlusion but also observe the changes in the skin as a function of time as water builds up in the SC. This occlusion response can be observed in parameters such as the amplitude of the reflected THz signal, marked as P in figure 5(b).

The decrease in the reflected signal as a function of time can be seen in figure 6, the first five seconds show the very high reflected values before the arm is placed on the window. The output from the pressure sensor is used to find the start of stable occlusion of the skin: this is the point at which the red dashed line fitting to the results begins. To account for the effects of occlusion when comparing results for different measurements, the reflected amplitude must be analysed at the same time into the occlusion process.

The quality of the contact between the skin and the imaging window can often vary throughout the 33 seconds of the measurement leading to occasional fluctuations in the occlusion trend. However, in order to meaningfully compare results at the same time into the occlusion process the data must be extrapolated to remove the effects of these fluctuations. To enable this, we fitted a biexponential function to the occlusion curve data (excluding outliers more than one

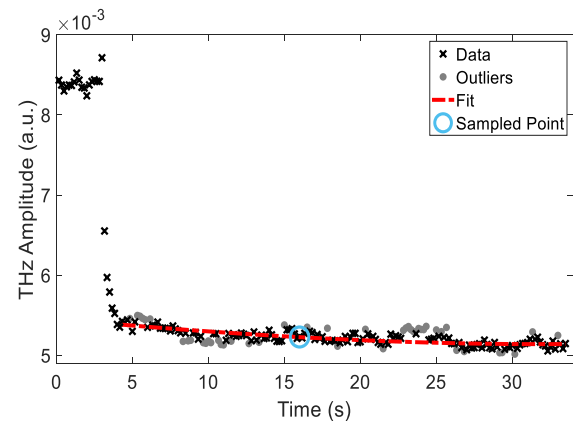


Figure 6. Processing the THz signal to remove fluctuations throughout the measurement caused by the subject moving or changing the contact pressure. Time dependent data was fit with a biexponential (red dashed line) and sampled 12 seconds into the occlusion process (blue circle). Measurements more than one standard deviation away from the fit (grey circles) were excluded and the fitting was repeated to improve stability.

standard deviation away from the original fit), as shown in figure 6 by the red dashed line [12]. The outliers which are excluded from the fitting are shown by grey circles. This makes it possible to extract a value for the THz measurement at a fixed time into the occlusion process without the potential for sampling at an anomaly, this is shown in the figure by the blue circle.

### 3.4 Data Processing

In addition to variables which may affect measurements of the skin if not carefully controlled, it is possible that the state of the skin will vary between measurements due to natural changes caused by eating, drinking or the time of day. It is not possible to prevent the skin changing in this way, instead processing techniques must be used to account for the effects. A variable called the normalised relative change (*NRC*) was defined in our previous work [15] and is stated in equation 5,

$$NRC(\%) = \frac{(X_{Tt} - X_{T0}) - (X_{Nt} - X_{N0})}{X_{T0} + (X_{Nt} - X_{N0})} \times 100, \quad (5)$$

where  $X_{Tt}$  is the measured parameter at time  $t$  following treatment with a sample and  $X_{T0}$  is the measured parameter of that same region of skin at  $t=0$ , before the skin was treated.  $X_{Nt}$  and  $X_{N0}$  are these same parameters for the region that was not treated; the difference between these two parameters acts as a representation of the natural variation of the skin between the measurements and is subtracted from the measured change in the treated region.

This approach to processing the measured responses can be applied to the results from both techniques used in this study, making it possible to compare the trends seen in response to the three different samples. By taking an average of the *NRC*s observed in each individual following treatment with a specific sample, an overall representation of the responses observed can be found. In this case, the standard deviation of

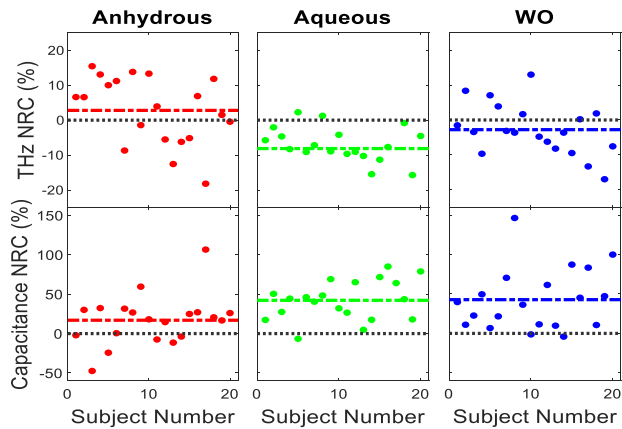


Figure 7. The normalised relative change measured in the THz amplitude and capacitance following treatment with each of the three samples. Each marker represents the individual response of a single subject, the coloured dashed line is the average response of the subjects to that sample and the grey dotted line is at zero.

the *NRC* across all subjects gives an indication of the range of the measured responses of subjects to a sample.

As the data from this study vary due to the changes in the initial state of skin and the way different subjects' skin will respond to the samples, a statistical test is required to see if the changes observed in the skin following treatment are statistically significant. First the data sets were checked using the Shapiro-Wilk test to confirm that the data can be modelled using a normal distribution which is a requirement for the further statistical tests to be valid [34]. Then the one-way ANOVA (Analysis of Variance) test is used with a 5% threshold to test whether the distributions of *NRC* responses to each sample are significantly different to one another. The Tukey-Kramer test is used to interpret the results of the ANOVA test and to ensure that the 5% significance threshold is maintained.

## 4. Results

### 4.1 Individual Trends

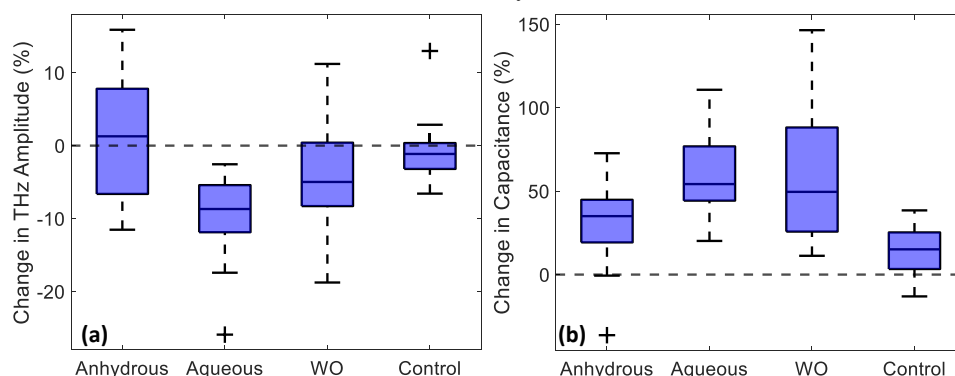


Figure 8. Box plots of the percentage change measured in (a) the reflected THz amplitude and (b) the capacitance for the three volar forearm regions following treatments with anhydrous, aqueous and WO samples and the change measured in the untreated control region. The top and bottom of the boxes indicate the 75<sup>th</sup> and 25<sup>th</sup> percentiles of the data, the whiskers mark the extent of the range of the data and the black crosses show any outliers.

The *NRC* for each individual 20 minutes after treatment with the samples, measured with both devices, is shown in figure 7. The dotted grey line marks the defined zero *NRC* point as a guide to the eye and the dashed coloured line is the average *NRC* for all the subjects for that treatment and device.

The clearest and most consistent change induced in the skin visible with both techniques is that following treatment with the aqueous sample shown in green. In the majority of subjects, the THz response decreases and corneometer response increases, both indicate an increase in the water content of skin.

The anhydrous and WO samples lead to a wider range of responses from the subjects in comparison, which can be seen from the distribution of the points about the coloured average line. The anhydrous response observed is a marginally positive *NRC* for both devices, but for THz there is a large variation as some subjects have a positive and others a negative *NRC* following treatment.

Treatment with the WO sample leads to an increase in the measured capacitance on a comparable level to the aqueous sample, although the distribution of the points about the average is much larger. The THz responses show a negative *NRC* following treatment with the WO sample, but again the distribution of the points is much larger compared to the aqueous sample with a range of positive and negative values, suggesting that subjects' skin responded in a range of ways to the oil-based samples but more consistently to the aqueous one.

### 4.2 Overall Results

A summary of the results is presented in figure 8 using box plots for the average percentage change in the THz and capacitance responses of skin. The centre lines through the boxes mark the median response for all subjects, with the horizontal edges of the boxes marking the 25<sup>th</sup> and 75<sup>th</sup> percentiles indicating the width of the distribution of responses. The whiskers on the box plots mark the upper and lower limits of the measurements and any outliers are shown by black crosses. Here the trends inferred from figure 7 are

clearer. For both techniques the distribution of the responses to the aqueous sample is the smallest, while there is a wider range of responses from the samples containing oil components. For some samples the average response is close to zero however, this is not because the most common response is no change following treatment with the sample; there are a range of responses to treatment with positive and negative values.

By studying the percentage change in this figure rather than *NRC* it is possible to also observe the change in the untreated region between the two measurements, giving an insight into the repeatability of the technique. Whilst we anticipate that there may be some natural variation in the untreated skin between measurements, these changes should be small compared to the changes induced by the treatments. For a technique with high repeatability between measurements we expect a percentage difference close to zero for the control region for the majority of subjects.

The THz responses shown in figure 8(a) follow what can be predicted using the optical properties of the samples relative to those of untreated skin, with the anhydrous sample increasing the reflected signal, the aqueous sample reducing it and the WO emulsion doing likewise but to a lesser extent. The large variation in responses particularly to the anhydrous sample could be explained by changes in the rate of absorption of the oily residue by different subjects' skin. The change in control region overlaps with the zero change line and has a much smaller range than the changes seen in response to the treatments. This confirms that the wide range of observed responses is caused by different skin responses to the samples, not a lack of repeatability in the THz measurements of the skin, this verifies the success of our robust protocol for *in vivo* THz measurements of the skin.

The capacitance measurements of the responses to the treatments shown in figure 8(b) show a positive average percentage change for all three samples, with very similar responses for the aqueous and WO samples, suggesting that the corneometer is not able to distinguish between samples of these types. The measured increase in hydration induced by the anhydrous sample is smaller than from the other two samples, it is possible that this could be caused by the oil on the surface of the skin interfering with the capacitance measurement. The capacitance measurements of the control region are close to zero and have a smaller range than the other samples, however this distinction is less obvious than in the THz measurements in figure 8(a), meaning that the THz measurements have the potential to be more repeatable than those taken with the corneometer.

With both devices it is possible to observe variation between subjects for each sample, as different skin types may react in a range of ways to the samples. This will be investigated further in section 4.5, where we discuss the

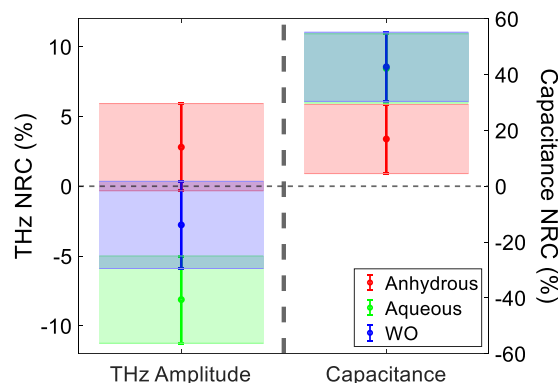


Figure 9. Results of performing the one-way analysis of variance test, showing the estimated mean of the distribution, the shaded error bars are the result of the Tukey-Kramer test, overlapping bars suggest that the changes observed are not statistically different. The left y axis corresponds to the normalised relative change in the amplitude of the reflected THz signal and the right y axis to the capacitance normalised relative change.

significance of the initial hydration state of the skin in determining the skin's response.

#### 4.3 Statistical Tests

The results of the ANOVA statistical testing are shown in figure 9, where the location of the dots mark the estimated mean of the distribution of responses to that treatment and the shaded error bars show the upper and lower confidence limits at a 95% level. Where these comparison intervals overlap, the two responses cannot be described as significantly different from one another, these results were obtained using the Tukey-Kramer test on the output of a one-way ANOVA test. This approach makes it possible to statistically compare the responses to treatments with all three samples measured with a certain technique to one another simultaneously.

The *NRC* of the THz responses in regions treated with the anhydrous and aqueous samples shown on the left of the figure by the red and green regions respectively, are found to be significantly different to one another. The THz response of skin to the WO sample was observed to be overlapping with the aqueous and anhydrous samples, which is unsurprising as the WO sample is a combination of the key components of the aqueous and anhydrous samples.

The responses measured by studying the capacitance of skin are quite different to the THz responses of skin, the WO and aqueous measurements are both significantly different to the response of the region treated with the anhydrous sample. However, the WO and aqueous regions overlap almost entirely suggesting that there is very little difference between the capacitance measurements for these two types of samples. The corneometer is primarily sensitive to changes in water content but less so to other changes in the skin, it appears that the aqueous and WO samples increase the water content by



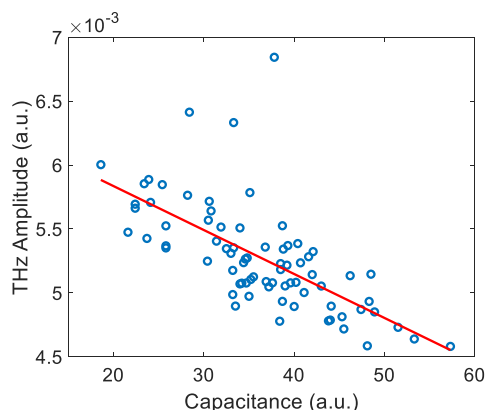


Figure 10. A demonstration of the correlation between the THz amplitude and capacitance measurements of untreated skin. The red line shows the line of best fit, correlation coefficient of  $r = -0.66$ .

similar amounts but no more can be learnt about the interaction of these samples with the skin.

#### 4.4 Correlation Testing

Figure 10 shows the THz amplitude measured in the four regions of untreated skin measured at the start of the study plotted against the capacitance measurements of the same regions. One subject was excluded from this study as it is thought that hair on the arms of the subject prevented good contact with the imaging window for the THz measurements. The correlation coefficient of the relationship between the THz amplitude and the capacitance is  $r = -0.66$ , this trend is negative as an increase in hydration is indicated by a decrease in the THz amplitude and an increase in capacitance.

#### 4.5 Effect of Initial Hydration of Skin on the Responses to the Samples

The measurements of the skin taken before treatment can be used to characterise the skin regions as dry or well hydrated. This initial state can influence the response of the region to the different treatments, to demonstrate this four

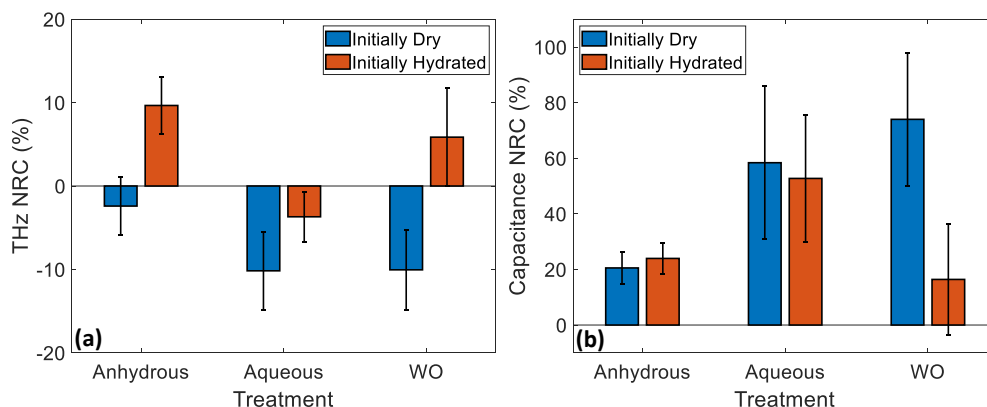


Figure 11. The normalised relative change following treatment with each of the samples measured with (a) the THz amplitude and (b) capacitance. The data is separated into the responses of subjects with initially dry and initially well hydrated skin shown by the blue and red bars respectively, with four subjects in each category. The error bars are the standard deviation of the responses from the four subjects in each group.

TABLE 3

Initially Dry		Initially Hydrated	
Capacitance (a.u.)	THz Amplitude* (a.u.)	Capacitance (a.u.)	THz Amplitude* (a.u.)
34.1	5.33	36.3	5.29
22.2	5.80	39.0	4.93
35.1	6.01	52.6	4.63
28.1	5.66	42.1	4.90

The initial hydration states of the eight subjects categorised as having dry or well hydrated skin before the study.

\*Factor of  $10^{-3}$  removed from values

subjects were chosen from each category as shown in table 3. Well hydrated skin was defined as having a capacitance value of over 36 and a reflected THz amplitude below  $5.3 \times 10^{-3}$  and the excluded region defines dry skin.

Figure 11 shows the NRC in the measured THz and capacitance responses of skin following treatment with each of the samples for the groups of subjects with initially dry or well hydrated skin, where the error bars are the standard deviation within each group.

In figure 11(a) the difference in the THz responses between the two groups is particularly clear for the oil-based samples. The increase in the THz response following treatment with oil-based samples in the well hydrated skin group could be caused by slow absorption of oil into the skin, meaning that an oily residue remains on the surface when the follow up measurements are taken 20 minutes later. The presence of oil on the surface of the skin is expected to increase the amplitude of the reflected THz pulse due to the increased difference between the refractive index of oil and the quartz window. However, for subjects with initially dry skin it is expected that their skin will quickly absorb the sample removing any oil from the surface, so the increase in the water content can be observed as a decreased THz amplitude. This difference in absorption rate can also explain the larger decrease in the THz amplitude in the dry skin group following treatment with the aqueous sample. It is possible that the aqueous sample will be

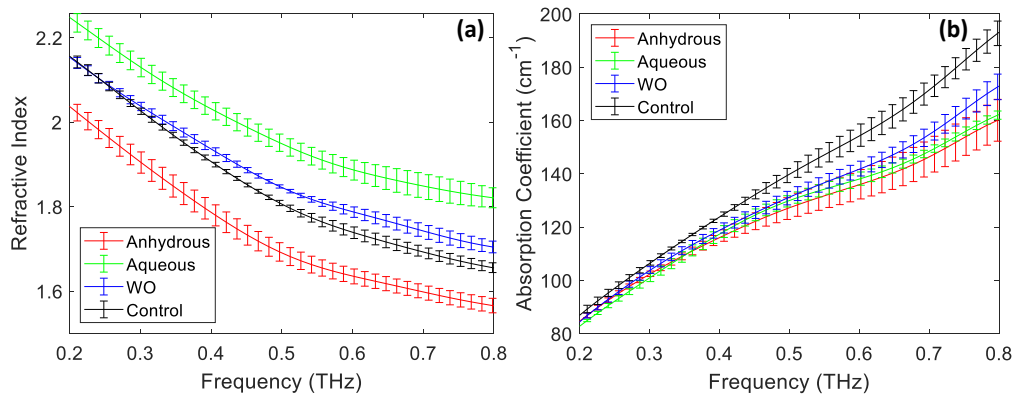


Figure 12. An example of (a) the refractive index and (b) the absorption coefficient of the skin following each of the treatment options for a single subject. The plotted values are the average of 5 consecutive results, the error bars are the standard deviation of these five results.

absorbed more rapidly by dry skin, meaning that a larger amount of water will be gained by the dry skin than the initially well hydrated skin, which may be slow to absorb the water allowing more of it to escape into the environment.

In comparison to the THz responses there is little difference in the capacitance measurements of dry and well hydrated skin responses to treatment with anhydrous and aqueous samples. There is however a difference in the responses to the WO sample; the initially dry skin shows a larger increase in capacitance than the well hydrated skin. It is suspected that the well hydrated skin may have some oil residue remaining on the skin surface at the time of measurement which could interfere with the capacitance measurement, reducing the perceived hydration of the skin. Whereas, the dry skin is less likely to have this oil on the skin surface, so the large increase in skin hydration can be seen in the capacitance measurement.

These results suggest that the initial hydration state of the skin can have a large effect on the way in which the skin responds to different samples and the time scale on which these changes occur. From the results shown in figure 11, it appears that measurements of the skin taken using THz imaging are more sensitive to these differences caused by the initial state and make it possible to infer more about the mechanisms of the interactions of the samples with the skin.

#### 4.6 Frequency Dependent Properties of the Skin

Finally, we present an example of the extracted refractive index and absorption coefficient for the skin following each of the treatment options in figure 12. This figure shows the changes in the frequency dependent properties for a single subject acquired 20 seconds into the occlusion process, the results from five consecutive repeat scans were averaged to give the measured results and the error bars are the standard deviation. It can be seen that the application of the samples has a more significant effect on the refractive index than the absorption coefficient. As with the time domain variable studied for the rest of this paper there is significant variation in the way different subjects' skin responds to the samples so

it is not meaningful to average these spectra to present the results for multiple subjects.

The technique for extracting these properties was explained in section 2.1.1, it is important to note that this approach assumes that the skin is a single homogeneous layer. This assumption may not be accurate after applying the products to the skin, but it gives an indication of the macroscopic changes occurring. Our future work will explore how to better model this more complex system.

## 5. Discussion

The effects of each sample can be discerned through the observations made in this study. Firstly, the aqueous sample had the most significant effect on the skin when measured with both devices. The corneometer observed an increase in the response from the skin as expected, due to its calibration using water to define the upper limit of possible responses. The THz reflection measurements showed a significant decrease following treatment with the aqueous sample, this observation has been seen in several other studies using treatments which increase the skin hydration, so was an expected result.

The effects of the anhydrous sample on the skin were more varied across the different subjects, it can be seen that the response could depend on the initial hydration state of the subject's skin. The capacitance measurements of the skin showed a slight increase following treatment with the anhydrous sample, indicating that the water levels had improved, but not as significantly as with the two other samples. This increase of water in the skin was caused by an occlusive layer trapping water inside the surface, but it is possible that the hydration increased more than this and the oily residue interfered with the measurement. The THz measurements showed an average increase in the reflected signal, caused by the presence of oil in the upper layers of the skin, though some subjects showed a decrease possibly because their skin has fully absorbed the oil so the resulting increase in hydration could be observed.

The treatment of the skin with the WO emulsion induced a range of responses across the subjects, which could also be associated with the initial hydration state of the skin. The WO sample is thought to most closely replicate the majority of commercial products with a mixture of both oil and water phases present. The THz measurements of the WO sample are not significantly different from the anhydrous and aqueous samples but lie between the two, which could be expected as the WO sample is some combination of the two. Whereas, the capacitance measurement of the WO sample on the skin is nearly identical to the response from the aqueous sample. This shows the difference in the way the measurements work, suggesting that both the WO and aqueous samples increase the water content of the skin by approximately the same amount.

It is possible to infer that the corneometer is an effective technique for evaluating skin hydration, while THz imaging can also be sensitive to the effects induced in the skin by a range of sample types. THz measurements were also more sensitive to the different responses to the samples observed by the hydrated and dry skin categories and was able to identify whether the oil had been completely absorbed. However, another technique to assess the surface lipids is needed to verify this hypothesis.

The correlation testing part of the study was carried out on untreated skin so that the presence of the samples on the skin did not influence the observations. The results show that there is moderate correlation between the techniques with  $r=-0.66$  [35]. Neither of the techniques measure the skin hydration directly but measure capacitance and THz reflectivity. Capacitance measurements of the skin are known to be affected by more than just skin hydration, so we would not predict perfect correlation between the two devices. The fact that there is moderate correlation with the current gold standard for measuring skin hydration suggests THz sensing has great potential for studying skin *in vivo*.

## 6. Conclusion

This study presents the first known comparison of *in vivo* measurements of human skin taken using THz TDS with the gold standard for skin hydration assessment, the corneometer which has known limitations. The measurements were taken of untreated skin as well as skin treated with three samples; aqueous, anhydrous and a WO emulsion. The corneometer is very sensitive to water content and shows the greatest changes, it can be most useful in studies where different levels of water are applied, however it is not able to distinguish between the WO and aqueous samples. The THz measurements compare well with this commercial technique, and the results are very positive for a relatively new technique. Some of the changes observed in the THz response were subtle and ways to enhance the contrast of these measurements should be sought. However, THz measurements came closer to distinguishing the responses of the three samples and shows a strong

sensitivity to the properties of the skin surface beyond hydration effects, as well as an ability to identify the different responses of dry and hydrated skin to the samples. Additionally, the study of the correlation between the techniques assists in the validation of THz *in vivo* imaging as a means of highly quantitative skin hydration assessment. It is hoped that with the expansion of this work through further modelling THz imaging could develop into a useful technique for skin surface characterisation beyond simple hydration measurements.

## Acknowledgments

This work was partially funded by the Engineering and Physical Sciences Research Council (EPSRC) (EP/S021442/1) and the Royal Society Wolfson Merit Award (EPM).

## Disclosures

The authors declare that there are no conflicts of interest related to this article. The datasets used in this work are available from

[https://figshare.com/articles/dataset/Evaluation\\_of\\_in\\_vivo\\_THz\\_Imaging\\_for\\_Assessing\\_Human\\_Skin\\_Hydration/12816311](https://figshare.com/articles/dataset/Evaluation_of_in_vivo_THz_Imaging_for_Assessing_Human_Skin_Hydration/12816311).

## Ethical Statement

The study was approved by the Biomedical Scientific Research Ethics Committee, BSREC, (REGO-2018-2273 AM03).

## References

- [1] Z. D. Taylor, R. S. Singh, D. B. Bennett, P. Tewari, C. P. Kealey, N. Bajwa, M. O. Culjat, A. Stojadinovic, H. Lee, J. P. Hubschman, E. R. Brown, and W. S. Grundfest, "THz medical imaging: In vivo hydration sensing," *IEEE Trans. Terahertz Sci. Technol.*, 2011, doi: 10.1109/TTHZ.2011.2159551.
- [2] G. G. Hernandez-Cardoso, S. C. Rojas-Landeros, M. Alfaro-Gomez, A. I. Hernandez-Serrano, I. Salas-Gutierrez, E. Lemus-Bedolla, A. R. Castillo-Guzman, H. L. Lopez-Lemus, and E. Castro-Camus, "Terahertz imaging for early screening of diabetic foot syndrome: A proof of concept," *Sci. Rep.*, vol. 7, no. 42124, 2017, doi: 10.1038/srep42124.
- [3] S. Fan, B. S. Y. Ung, E. P. J. Parrott, V. P. Wallace, and E. Pickwell-Macpherson, "In vivo terahertz reflection imaging of human scars during and after the healing process," *J. Biophotonics*, vol. 10, pp. 1143–1151, 2017, doi: 10.1002/jbio.201600171.
- [4] J. Wang, Q. Sun, R. I. Stantchev, T.-W. Chiu, A. T. Ahuja, and E. Pickwell-Macpherson, "In vivo terahertz imaging to evaluate scar treatment strategies: silicone gel sheeting," *Biomed. Opt. Express*, vol. 10, no. 7, pp. 3584–3590, 2019, doi: 10.1364/BOE.10.003584.

- [5] Z. D. Taylor, J. Garritano, S. Sung, N. Bajwa, D. B. Bennett, B. Nowroozi, P. Tewari, J. Sayre, J. P. Hubschman, S. Deng, E. R. Brown, and W. S. Grundfest, "THz and mm-wave sensing of corneal tissue water content: Electromagnetic modeling and analysis," *IEEE Trans. Terahertz Sci. Technol.*, vol. 5, no. 2, pp. 170–183, 2015, doi: 10.1109/TTHZ.2015.2392619.
- [6] Y. C. Sim, J. Y. Park, K.-M. Ahn, C. Park, and J.-H. Son, "Terahertz imaging of excised oral cancer at frozen temperature," *Biomed. Opt. Express*, vol. 4, no. 8, 2013, doi: 10.1364/BOE.4.001413.
- [7] R. M. Woodward, V. P. Wallace, R. J. Pye, B. E. Cole, D. D. Arnone, E. H. Linfield, and M. Pepper, "Terahertz pulse imaging of ex vivo basal cell carcinoma," *J. Invest. Dermatol.*, 2003, doi: 10.1046/j.1523-1747.2003.12013.x.
- [8] P. C. Ashworth, E. Pickwell-MacPherson, E. Provenzano, S. E. Pinder, A. D. Purushotham, M. Pepper, and V. P. Wallace, "Terahertz pulsed spectroscopy of freshly excised human breast cancer," *Opt. Express*, vol. 17, no. 15, p. 12444, 2009, doi: 10.1364/OE.17.012444.
- [9] J. Wang, H. Lindley-Hatcher, K. Liu, and E. Pickwell-MacPherson, "Evaluation of transdermal drug delivery using terahertz pulsed imaging," *Biomed. Opt. Express*, vol. 11, no. 8, pp. 4484–4490, 2020, doi: 10.1364/boe.394436.
- [10] D. I. Ramos-Soto, A. K. Singh, E. Saucedo-Casas, E. Castro-Camus, and M. Alfaro-Gomez, "Visualization of moisturizer effects in stratum corneum in vitro using THz spectroscopic imaging," *Appl. Opt.*, vol. 58, no. 24, pp. 6581–6585, 2019, doi: 10.1364/AO.58.006581.
- [11] H. J. Liebe, G. A. Hufford, and T. Manabe, "A model for the complex permittivity of water at frequencies below 1 THz," *Int. J. Infrared Millimeter Waves*, vol. 12, no. 7, pp. 659–675, 1991.
- [12] Q. Sun, E. P. J. Parrott, Y. He, and E. Pickwell-MacPherson, "In vivo THz imaging of human skin: Accounting for occlusion effects," *J. Biophotonics*, vol. 11, no. 2, p. e201700111, 2018, doi: 10.1002/jbio.201700111.
- [13] J. Wang, R. I. Stantchev, Q. Sun, T.-W. Chiu, A. T. Ahuja, and E. Pickwell-Macpherson, "THz in vivo measurements: the effects of pressure on skin reflectivity," *Biomed. Opt. Express*, vol. 9, no. 12, pp. 6467–6476, 2018.
- [14] M. Denda and T. Tsuchiya, "Barrier recovery rate varies time-dependently in human skin," *Br. J. Dermatol.*, vol. 142, no. 5, pp. 881–884, 2000, doi: 10.1046/j.1365-2133.2000.03466.x.
- [15] H. Lindley-Hatcher, A. I. Hernandez-Serrano, Q. Sun, J. Wang, J. Cebrian, L. Blasco, and E. Pickwell-Macpherson, "A Robust Protocol for In Vivo THz Skin Measurements," *J. Infrared, Millimeter, Terahertz Waves*, vol. 40, no. 9, pp. 980–989, 2019.
- [16] E. Berardesca, M. Loden, J. Serup, P. Masson, and L. M. Rodrigues, "The revised EEMCO guidance for the in vivo measurement of water in the skin," *Ski. Res. Technol.*, vol. 24, no. 3, pp. 351–358, 2018, doi: 10.1111/srt.12599.
- [17] Q. Sun, R. I. Stantchev, J. Wang, E. P. J. Parrott, A. Cottenden, T.-W. Chiu, A. T. Ahuja, and E. Pickwell-MacPherson, "In vivo estimation of water diffusivity in occluded human skin using terahertz reflection spectroscopy," *J. Biophotonics*, vol. 12, no. 2, p. e201800145, 2019, doi: 10.1002/jbio.201800145.
- [18] X. Chen, E. P. J. Parrott, B. S. Y. Ung, and E. Pickwell-Macpherson, "A Robust Baseline and Reference Modification and Acquisition Algorithm for Accurate THz Imaging," *IEEE Trans. Terahertz Sci. Technol.*, vol. 7, no. 5, pp. 493–501, 2017, doi: 10.1109/TTHZ.2017.2722981.
- [19] J. D. E. McIntyre and D. E. Aspnes, "Differential reflection spectroscopy of very thin surface films," *Surf. Sci.*, vol. 24, no. 2, pp. 417–434, 1971, doi: 10.1016/0039-6028(71)90272-X.
- [20] D. Grischkowsky, S. Keiding, M. van Exter, and C. Fattinger, "Far-infrared time-domain spectroscopy with terahertz beams of dielectrics and semiconductors," *J. Opt. Soc. Am. B*, vol. 7, no. 10, p. 2006, 1990, doi: 10.1364/josab.7.002006.
- [21] M.-M. Constantin, E. Poenaru, C. Poenaru, and T. Constantin, "Skin Hydration Assessment through Modern Non-Invasive Bioengineering Technologies," *Maedica (Buchar)*, vol. 9, no. 1, pp. 33–38, 2014.
- [22] Courage-Khazaka, "Corneometer® CM 825 Courage + Khazaka electronic GmbH." <http://www.courage-khazaka.de/index.php/en/products/scientific/55-corneometer> (accessed Mar. 27, 2020).
- [23] J. M. Crowther, "Understanding effects of topical ingredients on electrical measurement of skin hydration," *Int. J. Cosmet. Sci.*, vol. 38, no. 6, pp. 589–598, 2016, doi: 10.1111/ics.12324.
- [24] K. C. Madison, "Barrier function of the skin: 'La Raison d'Être' of the epidermis," *J. Invest. Dermatol.*, vol. 121, no. 2, pp. 231–241, 2003, doi: 10.1046/j.1523-1747.2003.12359.x.
- [25] R. M. Law, M. A. Ngo, and H. I. Maibach, "Twenty Clinically Pertinent Factors/Observations for Percutaneous Absorption in Humans," *Am. J. Clin. Dermatol.*, vol. 21, no. 1, pp. 85–95, 2020, doi: 10.1007/s40257-019-00480-4.
- [26] M. A. Ngo, M. O'Malley, and H. I. Maibach, "Percutaneous absorption and exposure assessment of pesticides," *J. Appl. Toxicol.*, vol. 30, no. 2, pp. 91–114, 2010, doi: 10.1002/jat.1505.
- [27] M. Hoppel, K. Kwizda, D. Baurecht, M. Caneri, and C. Valenta, "The effect of a damaged skin barrier on percutaneous absorption of SDS and skin hydration investigated by confocal Raman spectroscopy," *Exp. Dermatol.*, vol. 25, no. 5, pp. 390–392, 2016, doi: 10.1111/exd.12950.
- [28] N. Lu, P. Chandar, D. Tempesta, C. Vincent, J. Bajor, and H. McGuinness, "Characteristic differences in barrier and hygroscopic properties between normal and cosmetic dry skin. I. Enhanced barrier analysis with sequential tape-stripping," *Int. J. Cosmet. Sci.*, vol. 36, no. 2, pp. 167–174, 2014, doi: 10.1111/ics.12112.
- [29] S. Verdier-Sévrain and F. Bonté, "Skin hydration: A review on its molecular mechanisms," *J. Cosmet. Dermatol.*, vol. 6, no. 2, pp. 75–82, 2007, doi: 10.1111/j.1473-2165.2007.00300.x.
- [30] S. A. Ventura and G. B. Kasting, "Dynamics of glycerine and water transport across human skin from binary mixtures," *Int. J. Cosmet. Sci.*, vol. 39, no. 2, pp. 165–178, 2017, doi: 10.1111/ics.12362.
- [31] J. W. Fluhr, R. Darlenski, and C. Surber, "Glycerol and the skin: Holistic approach to its origin and functions," *Br. J. Dermatol.*, vol. 159, no. 1, pp. 23–34, 2008, doi: 10.1111/j.1365-2133.2008.08643.x.
- [32] M. D. A. Van Logtestijn, E. Domínguez-Hüttinger, G. N. Stamatias, and R. J. Tanaka, "Resistance to water diffusion in the stratum corneum is depth-dependent," *PLoS One*, vol. 10, no. 2, pp. 1–12, 2015, doi: 10.1371/journal.pone.0117292.
- [33] C. W. Blichmann, J. Serup, and A. Winther, "Effects of



- single application of a moisturizer: Evaporation of emulsion water, skin surface temperature, electrical conductance, electrical capacitance, and skin surface (emulsion) lipids," *Acta Derm. Venereol.*, vol. 69, no. 4, pp. 327–330, 1989, doi: 10.2340/0001555569327330.
- [34] S. S. Shapiro and M. B. Wilk, "An Analysis of Variance Test for Normality ( Complete Samples )," *Biometrika*, vol. 52, no. 3/4, pp. 591–611, 1965.
- [35] M. M. Mukaka, "Statistics corner: A guide to appropriate use of correlation coefficient in medical research," *Malawi Med. J.*, vol. 24, no. 3, pp. 69–71, 2012.